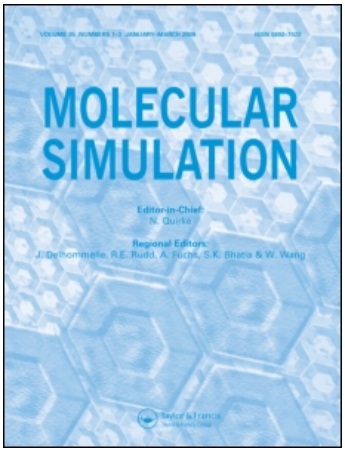

Molecular Simulation
Publication details, including instructions for authors and subscription information:
http://www.informaworld.com/smpp/title~content=t713644482

Study of structural and thermodynamic properties of GaAs and InAs using Monte Carlo simulations

J. Adhikari[a]; A. Kumar[a]
[a] Department of Chemical Engineering, India Institute of Technology Bombay, Mumbai, India

To cite this Article Adhikari, J. and Kumar, A.(2007) 'Study of structural and thermodynamic properties of GaAs and InAs using Monte Carlo simulations', Molecular Simulation, 33: 8, 623 — 628
To link to this Article: DOI: 10.1080/08927020701365505
URL: http://dx.doi.org/10.1080/08927020701365505

Molecular Simulation, Vol. 33, No. 8, July 2007, 623–628

Study of structural and thermodynamic properties of GaAs and InAs using Monte Carlo simulations

J. ADHIKARI* and A. KUMAR†

Department of Chemical Engineering, India Institute of Technology Bombay, Mumbai 400076, India

(Received March 2007; in final form March 2007)

Binary compound semiconductor alloys such as GaAs and InAs find extensive use in our daily lives. This study predicts the structural and thermodynamic properties such as the lattice constant, linear thermal expansion coefficient, nearest neighbour distances and molar heat capacities at constant volume, and their variations with temperature using Monte Carlo simulations. The Tersoff potential model is used to describe the interatomic interactions and the model is validated by comparing the predicted properties against experimental data for GaAs. The simulation results for the GaAs alloy show good agreement with literature data for lattice constant and bond length measurements. Linear thermal expansion coefficients are overestimated consistently as compared to experimental data for all temperatures. Low temperature range thermal expansion coefficient data capture qualitative behaviour but is unable to accurately predict quantitative data. The specific heat at constant volume measured at high temperatures follows the Dulong–Petit law. Having established the validity of the Tersoff potential in modelling III–V binary alloys, the same properties and their variance with temperature are determined for the InAs alloy.

Keywords: GaAs; InAs; Tersoff potential; Monte Carlo method

1. Introduction

Gallium Arsenide (GaAs) and Indium Arsenide (InAs) are examples of III–V compound semiconductor alloys, which find extensive application in the manufacture of electronic devices. GaAs crystallizes in the zinc blende structure at 300 K with an energy band gap of 1.43 eV and a lattice constant of 5.6534 Å [1]. The aim of this study is to predict the structural and thermodynamic properties of GaAs and InAs, and compare the simulation results with available literature values. In this study, we utilize the Tersoff potential energy function (PEF) to model the interatomic interactions in this binary alloy. Monte Carlo simulations are conducted to determine thermo-physical properties such as lattice constants, linear thermal expansion coefficients (α_T) and nearest neighbour (NN) distances at different temperatures up to the melting point. The molar heat capacity at constant volume (C_V) is also determined at high temperatures. Considering that some of these properties have been determined experimentally for GaAs, a comparison of simulation results with available experimental data will validate the Tersoff model as a realistic model for compound semiconductor alloy systems. This model is then applied to determine the same properties for the InAs alloy. Various studies based on the Tersoff PEF have calculated the potential parameters specific to Si, Ge, C, SiC, SiGe, BAs, GaN and AlN by fitting to experimental data [2–7]. Ashu *et al.* [8] have shown that, apart from binary alloys, the Tersoff model can also be applied to ternary alloys such as InGaAs. Nakamura *et al.* [9] have attempted to modify the Tersoff PEF, incorporating Coulumbic contributions to account for the ionicity of the compounds.

Experimental studies have been conducted to investigate the behaviour of GaAs at different temperature conditions. Novikova has investigated the low temperature linear expansion coefficient behaviour of GaAs in the temperature range of 28–348 K [10]. At 300 K, the lattice constant has been determined experimentally by Driscoll *et al.* to be 5.65325 ± 0.00002 Å [1]. The normal melting point was found to be 1513 ± 1 K by Lichter and Sommelet [1]. Blakemore has reported the change in length in the

*Corresponding author. Tel.: + 91-22-25767245. Fax: + 91-22-25726895. Email: adhikari@che.iitb.ac.in
†Dual degree student graduated in July, 2006. Email: kumar.atul@gmail.com

Molecular Simulation
ISSN 0892-7022 print/ISSN 1029-0435 online © 2007 Taylor & Francis
http://www.tandf.co.uk/journals
DOI: 10.1080/08927020701365505

range of 200–1000 K and also the value of α_T in the same temperature range. In the lower temperature range of 120–350 K, the α_T values are again given by Blakemore. The same author also shows from Lichter and Sommlet's values of specific heats that for high temperatures, from 300 K to the melting point of GaAs, $C_V \rightarrow 3R$ [1]. As experimental data is available extensively for GaAs, we have compared our simulations for GaAs to this data and thus, test the validity of the Tersoff PEF. We have then used this PEF to model the behaviour of the InAs alloy. We investigated two sets of parameters for the InAs system to determine the best possible results by comparing with experimental data available at 300 K.

In this paper, we report the results of structural and thermodynamic properties of GaAs and InAs, arrived at, through Monte Carlo simulation. These results have been compared with literature data where available. All other studies by other authors mentioned have been conducted using molecular dynamics. Monte Carlo simulations have been used to study the miscibility characteristics in the III–V semiconductor alloys previously using the Valence Force Field potential model by Adhikari and Kofke [11,12]. The paper is organized such that, in Section II a description of Tersoff PEF is presented. Section III presents the simulation method. In Section IV, simulation results and its comparison with experimental data have been presented and prediction has been made for properties of InAs. Finally, a general conclusion follows in the last section.

2. Potential model

Tersoff proposed a new empirical PEF for covalently bonded solids such as elemental semiconductors and their mixtures [2–4]. This model is based on the fact that the strength of a bond (i.e. bond order) depends on the local environment (i.e. coordination number). Most predominantly covalent systems have open structures, as an atom with fewer neighbours will form stronger bonds as compared to a close-packed structure where an atom has many neighbours. Tersoff states that the energy is modelled as a sum of pair-like interactions, where, however the coefficient of the attractive term in the potential (which plays the role of bond order) depends on the local environment, giving a many-body potential. Compound semiconductors are predominantly covalent systems showing tetrahedral arrangement of atoms. Hence, other authors extended this PEF to model these compound semiconductor alloys [5,6,8,13]. The III–V alloys have some ionic characteristics [9]. For the purpose of this study, the computational costs involved including Coulumbic interactions far outweighs any contribution to the accuracy of the results. Tersoff himself showed, his PEF to be both transferable and accurate for SiC which has ionic characteristics in the rock salt configuration as well as the cubic form [4].

The mathematical form of the Tersoff potential model for multi-component system [4] is as follows:

$$E = \sum_i E_i = \frac{1}{2}\sum_{i \neq j} V_{ij} \tag{1}$$

$$V_{ij} = f_c(r_{ij})[a_{ij} f_R(r_{ij}) + b_{ij} f_A(r_{ij})] \tag{2}$$

$$f_R(r_{ij}) = A_{ij}\exp(-\lambda_{ij} r_{ij}) \tag{3}$$

$$f_A(r_{ij}) = -B_{ij}\exp(-\mu_{ij} r_{ij}) \tag{4}$$

$$f_C(r_{ij}) = \begin{cases} 1.0, & r_{ij} < R_{ij}; \\ \frac{1}{2} + \frac{1}{2}\cos\left[\frac{\pi(r_{ij} - R_{ij})}{(S_{ij} - R_{ij})}\right], & R_{ij} < r_{ij} < S_{ij}; \\ 0.0, & r_{ij} > S_{ij} \end{cases} \tag{5}$$

$$b_{ij} = \left(1 + \beta_{ij}^{n_{ij}} \zeta_{ij}^{n_{ij}}\right)^{-1/2n_{ij}} \tag{6}$$

$$\zeta_{ij} = \sum_{k \neq i,j} f_C(r_{ij}) g(\theta_{ijk}) \tag{7}$$

$$g(\theta_{ijk}) = 1 + \frac{c_i^2}{d_i^2} - \frac{c_i^2}{\left[d_i^2 + (h_i - \cos\theta_{ijk})^2\right]} \tag{8}$$

In equation (1), E is the total energy of the system, E_i is the i^{th} site energy and V_{ij} is the bond energy. The repulsive pair potential is represented by f_R and is defined as in equation (3). f_A represents the attractive pair potential associated with bonding, which is defined in equation (4). Equation (5) shows the smooth cut-off function, f_C, which assures that the cut-off dies off to zero smoothly. The bond order parameter b_{ij} is defined as per equation (6) and describes the effect of neighbouring atoms (represented by index k) on the bond-formation energy. This is the parameter that makes the potential a many-body PEF. Equation (7) counts the number of bonds to atom i except the ij bond and gives the effective coordination number ζ_{ij}. For the cut-off function, values of R and S are chosen such that only the first shell of neighbours are included, the effective coordination number tends to be the value of the coordination number minus one. The parameter n_{ij} quantifies the measure by which the closer neighbours are preferred over more distant ones in the competition to form bonds. The bond angle between bonds ij and ik is given by θ_{ijk} and the interatomic distance by r_{ij}. Here, A_{ij}, B_{ij}, λ_{ij}, μ_{ij}, R_{ij}, S_{ij}, β_{ij}, n_{ij}, c_i, d_i and h_i are fitting parameters defined in table 1.

3. Simulation method and details

The Monte Carlo simulations to estimate lattice constant and NN distance are conducted in the isothermal isobaric (N, P, T) ensemble where the pressure P, temperature T and particle number N are kept fixed and the volume V is allowed to vary. The initial configuration is taken to be the cubic zinc blende structure. The pressure values are held constant at 1 bar. System sizes of $N = 64$ and $N = 216$ are considered for a wide range of temperature values below

Table 1. Parameters of the potential used in the simulations. All parameters are taken from Ashu *et al.* (reference 1) except In–As parameters which are taken from reference 11.

Parameter	*Units*	*As–As*	*In–Ga*	*In–In*	*In–As*	*Ga–Ga*	*Ga–As*
A_{ij}	(eV)	1571.86	1214.917	2975.54	1968.295443	993.88	2579.46
B_{ij}	(eV)	546.431	177.22	360.61	266.571631	136.123	317.21
λ_{ij}	(Å^{-1})	2.38413	2.5621	2.6159	2.597556	2.50842	2.82805
μ_{ij}	(Å^{-1})	1.72872	1.58600	1.68117	1.422429	1.49082	1.72303
R_{ij}	(Å)	3.4	3.4	3.4	3.5	3.4	3.4
S_{ij}	(Å)	3.6	3.6	3.6	3.7	3.6	3.6
β_{ij}		0.007488	0.70524	2.10871	0.3186402	0.23586	0.35719
n_{ij}		0.60879	3.43739	3.40223	0.7561694	3.47290	6.31747
c_i		5.27313	0.080256	0.084215	5.172421	0.076297	1.22630
di		0.75102	195.2950	19.2626	1.665967	19.7964	0.79040
h_i		0.15292	7.26910	7.39228	−0.5413316	7.14591	−0.51848

the melting point. For the $N = 64$ system size, simulations were carried out for 100,000 relaxation cycles and 100,000 production cycles. In the case of the larger system, 35,000 equilibration cycles and the same number of production cycles was found to be adequate at temperatures above 100 K. For lower temperatures (less than 100 K), the production cycles were increased to 70,000 cycles while keeping the relaxation cycles the same. This simulation method involves trial atom displacement and trial volume changes with the cycle frequency ratio being 1:1 such that, one cycle of atom displacement moves involves N steps. The average volumes are determined as a function of temperature in these simulations. From the average volume data, the lattice constant can be determined as $V = (na)^3$ where a is the lattice constant and n is the number of unit cells along the length of the simulation box. The linear thermal expansion coefficient, is determined using the following equation (9)

$$\alpha_T = \frac{1}{a}\frac{\partial a}{\partial T}\bigg|_P \tag{9}$$

Determination of the molar heat capacity at constant volume is done in the canonical (N, V, T) ensemble where the volume V, temperature T and particle number N are kept fixed and the pressure P is allowed to vary. In this ensemble, the simulation method involves atom displacement trials only, with volume of the simulation box at temperature T set from the volume measured in the (N, P, T) simulation previously described. The average potential energy $\langle U \rangle$ is determined and the internal energy U_{internal} of the system is determined as shown in equation (10)

$$U_{\text{internal}} = \langle E \rangle = \langle U \rangle + \frac{3}{2}NkT \tag{10}$$

The specific heat at constant volume is determined as the slope of the internal energy versus temperature graph as per equation (11)

$$C_V = \frac{\partial U_{\text{internal}}}{\partial T}\bigg|_V = \frac{\partial \langle E \rangle}{\partial T}\bigg|_V \tag{11}$$

4. Results and discussion

4.1 Lattice constant

4.1.1 GaAs. The simulations in the (N, P, T) ensemble were carried out for two temperature ranges, namely, a low temperature range of 10–90 K, and a high temperature range from 100 to 900 K which is lower than the melting point of the GaAs solid. Figure 1A indicates the variation of lattice constant, $a(T)$ measured in Å, with temperature. Figure 1A shows good agreement of lattice constant values obtained by our simulations with experimental data reviewed by Blakemore for the higher temperature range. In the high temperature range (100–900 K), comparison of the lattice constant values demonstrates that the maximum deviation of simulation results from experimental data is 0.55% at the highest temperature considered, 900 K. Simulations were carried out for two different system sizes (i.e. $N = 64$ and $N = 216$) to study finite size effects. The simulation values for the two system sizes were found to deviate by a maximum of 0.006% indicating that finite size effects are negligible. The value of lattice constant determined from simulation at 300 K is compared with literature data in table 2.

4.1.2 InAs. The same simulation method as in the case of GaAs was used to predict the lattice constant behaviour of InAs in a low temperature range of 10–90 K, and a high temperature range of 100–900 K. Simulations were conducted for two system sizes, namely, $N = 64$ atoms and $N = 216$ atoms, for the temperature range 100–700 K, and for the points thereafter only the smaller system size was considered, as shown in figure 1B. In the low temperature range, the maximum deviation in the values of the lattice constants determined from simulations of the two different system sizes is 0.001%. For the high temperature range, the deviation is a maximum of 0.001% at a temperature of 700 K. Thus, we can conclude that the finite size effects are insignificant. Simulations were conducted using two sets of parameters, one from Ashu *et al.*, and the other from Nordlund. Our simulations showed a better agreement of simulation results with the experimental data point available at 300 K (6.058 Å) [14]

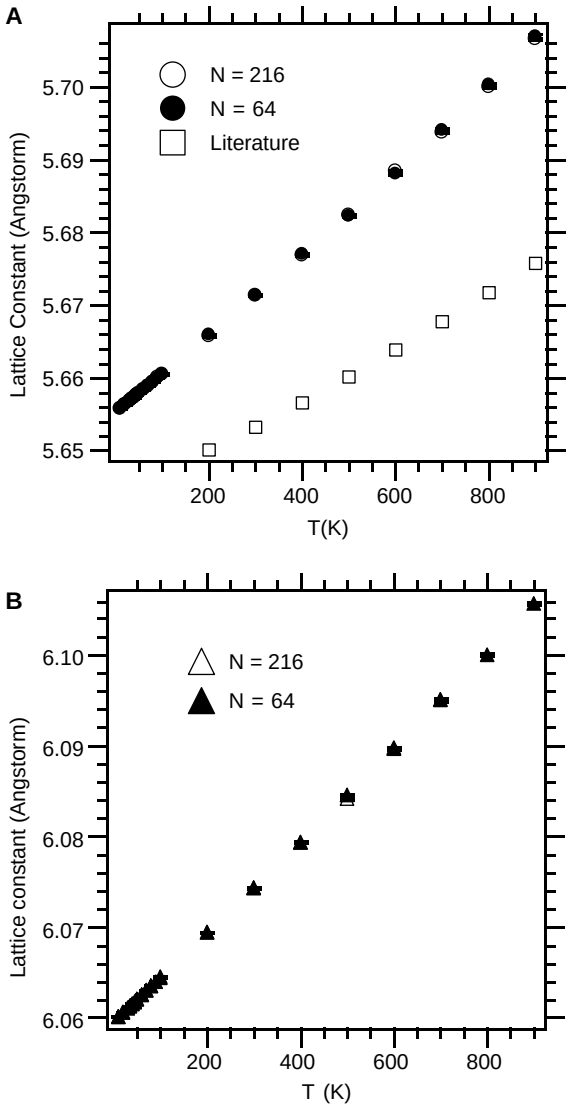

Figure 1. (A) Plot of lattice constant of GaAs as a function of temperature. The circle shaped markers indicate the simulation results and the square markers show the literature data from reference 1. The values for the two system sizes ($N = 64$ and $N = 216$) coincide, leaving only the shaded markers for the $N = 64$ atoms system results visible. (B) Plot of lattice constant of InAs as a function of temperature.

Table 2. Comparison of property data obtained from simulation with literature data at 300 K. Number in parenthesis indicates error in the last decimal place. Literature data for GaAs is from reference 1. References for literature data for InAs are given in square brackets.

Property	*Simulation*	*Literature*
GaAs lattice constant (Å)	5.67137 (8)	5.65325 (2)
Bond length Ga–As (Å)	2.45890 (4)	2.44793
GaAs linear thermal expansion coefficient (K^{-1})	9.53E-6	5.73E-6
InAs lattice constant (Å)	6.074 (35)	6.058[14]
Bond length In–As (Å)	2.63455 (4)	2.623[16]
InAs linear thermal expansion coefficient (K^{-1})	8.31E-6	–

with Norlund's parameters for In–As interaction (6.0744 Å) as compared to that reported by Ashu *et al.* (5.836 Å) The comparison of simulation data with experimental data at 300 K is shown in table 2.

4.2 Linear thermal expansion coefficient

4.2.1 GaAs. The data for the lattice constant as a function of temperature is fit to a polynomial expression and is differentiated with respect to temperature as in equation (9) to generate the values for the linear thermal expansion coefficient, α_T, for the range of temperatures considered in the lattice constant calculations. Figure 2 indicates the behaviour of the expansion coefficient with temperature for the high temperature range (100–900 K). Compared to the experimental value of expansion coefficient at 300 K, 5.73E-6 K^{-1} the simulation value is 9.53E-6 K^{-1} as shown in table 2. As finite size effects can be ignored, the simulation data shown in figure 2 is for the $N = 64$ system size. The values are of the same order as for known literature data which are also illustrated in the same figure.

At low temperatures, semiconductors show anomalous linear thermal expansion coefficient values, as verified by Spark and Swenson [15] and Novikova [10], through their experimental studies. The low temperature simulation results show a qualitatively similar behaviour, where for the 10–60 K temperature range we have a decreasing expansion coefficient followed by an increasing upwards slope, as illustrated in figure 3A. The Tersoff PEF is able to capture this behaviour though the quantitative values are not the same. Spark and Swenson have shown experimentally that the linear thermal expansion coefficients decrease until approximately 30 K and then increase as temperature increases. Novikova determined the α_T

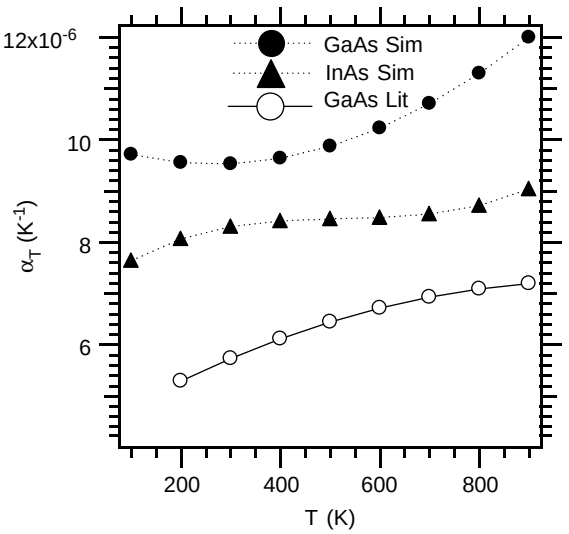

Figure 2. Plot of linear thermal expansion coefficient of GaAs and InAs as a function of temperature in the high temperature range (100–900 K). The circle shaped shaded markers indicate the simulation results and the circle shaped open markers show the experimental data for GaAs from reference 1. The line is a guide to the eye. InAs simulation data are represented by shaded triangles.

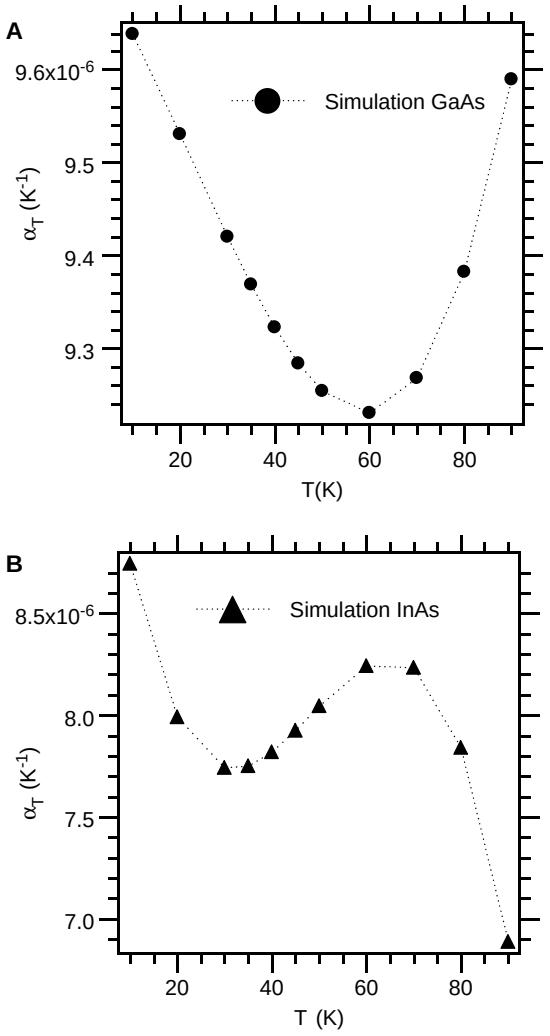

Figure 3. (A) Plot of linear thermal expansion coefficient of GaAs as a function of temperature in the low temperature range. Results shown are for $N = 64$ atoms system size. (B) Plot of linear thermal expansion coefficient of InAs as a function of temperature in the low temperature range. Results shown are for $N = 64$ atoms system size.

values to be negative for $T < 56$ K, which is not the case for our simulation data. Figure 3A shows simulation results for system size of $N = 64$ atoms. The simulation results consistently overestimate the value for linear thermal expansion coefficient for the low temperature range.

4.2.2 InAs. A similar behaviour for α_T has been predicted for InAs whereby for a temperature below 60 K the values of α_T are found to show the characteristic kick, as seen in figure 3B. Sparks and Swenson determined experimentally that α_T while negative for temperature between 14 and 40 K, also decreases up to approximately 30 K, and then increases [15]. Again, the Tersoff PEF is able to capture qualitatively correct behaviour, though overestimating the quantitative values. The high temperature α_T behaviour in the range of 100–900 K is predicted and shown in figure 2.

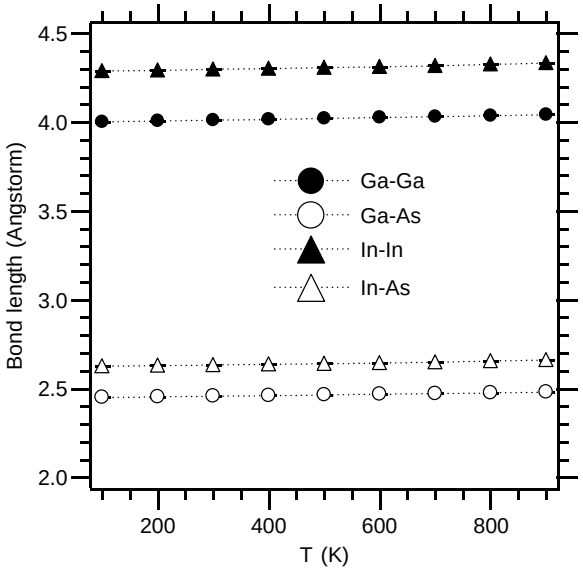

Figure 4. Plot of the NN interatomic distance between constituent atoms as a function of temperature. Results shown are for $N = 64$ atoms system size. Statistical error is smaller than the symbol size.

4.3 Bond length

4.3.1 GaAs. The term bond length refers to the average distance between the two neighbouring atoms of different species, i.e. NN distance Ga-As and the distance between nearest atoms of the same species Ga–Ga. Figure 4 shows the behaviour of NN distance between Gallium and Arsenide atoms in the binary alloy for the temperature range 100–900 K. At 300 K, compared to the ideal NN distance (i.e. $\sqrt{3}a/4$ where a is the lattice constant at 300 K) of 2.456 Å, the value obtained from simulations is 2.459 Å, as also summarized in table 2. Figure 4 also includes a plot of the Ga–Ga bond length and the average distance between the Gallium atoms in the first shell is found to be 4.0128 Å at 300 K. Figure 4 shows simulation results for $N = 64$ atoms only.

4.3.2 InAs. Figure 4 shows the NN distances for In–In and the same for In–As bond lengths for the temperature range 100–900 K. The value of the In–In and In–As distances at 300 K are 4.2988 Å and 2.63455 Å. Figure 4 shows simulations for $N = 64$ atoms only.

4.4 Molar heat capacity at constant volume

4.4.1 GaAs. Figure 5 illustrates the variation of internal energy with temperature for the range 500–900 K and for the $N = 64$ system size. Experimental data in this temperature range shows that the molar heat capacity is almost constant, C_v, and has a value of $3R$ where R is the universal gas constant. Molar heat capacity at constant volume is obtained from the slope of the straight line equation obtained by fitting to the internal energy versus temperature plot is estimated to be 24.991 J/mol K. This values indicates that the Dulong–Petit law is obeyed by

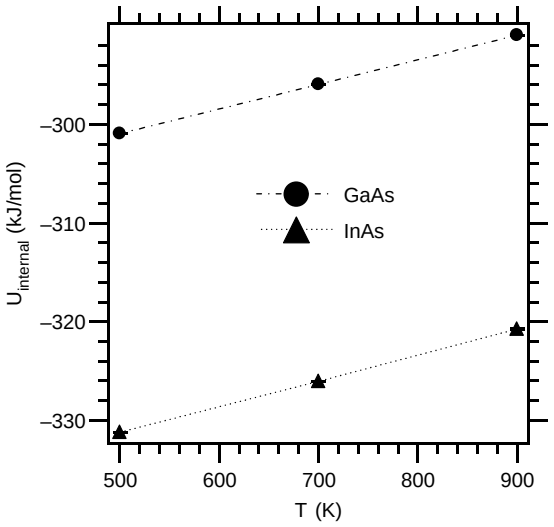

Figure 5. Plot of the internal energy in kJ/mol as a function of temperature in *K*. Results shown are for $N = 64$ atoms system size. The lines are an aid to the eye. Statistical error is smaller than the symbol size.

this solid at high temperatures, where according to the law $C_V = 3 \times 8.314$ J/mol $K = 24.94$ J/mol K. Thus, the Tersoff PEF is able to predict the behaviour of the GaAs solid at high temperatures.

4.4.2 InAs. The molar heat capacity, C_V, at high temperatures, 500–900 K, is determined and the value is found to be 26.148 J/mol K which is close to the value predicted by the Dulong–Petit law.

5. Conclusions

Comparison of data at the two system sizes investigated, viz. $N = 64$ and $N = 216$, for GaAs and InAs have shown that finite size effects are negligible. Table 2 gives a comparison of literature values of the structural properties of GaAs at 300 K with those obtained from simulations. There is a good agreement between the two sets of values. For low temperature range, the Tersoff PEF while unable to predict the quantitative results accurately is able to qualitatively capture the anomalous behaviour of the linear thermal expansion values which initially show a decrease with increasing temperature before returning to expected behaviour of the α values increasing as temperature rises beyond 100 K for both the binary alloys. For high temperatures, the results for the lattice constant from literature and our simulation results show a remarkable concurrence for GaAs system. The NN Ga–As interatomic distance at 300 K shows an insignificant difference between our simulation result and the ideal distance indicated in literature. The bond lengths In–In and In–As are predicted.

The Tersoff PEF also shows that at high temperatures, the C_V value obeys the Dulong–Petit Law which is reflected in the experimental data for the same temperature range. We have predicted the structural and thermodynamic properties of GaAs alloy using Monte Carlo simulation and compared with experimental data where available. Thereby, we have been able to study the limitations of the assumed PEF and we have been able to establish the validity of the Tersoff PEF in modelling binary compound semiconductor alloys such as GaAs. This PEF is then used to predict the properties of the InAs system and are reported here.

Acknowledgements

Computational resources have been provided by Computer Centre at Indian Institute of Technology Bombay and funding for the project is provided by the Department of Science and Technology, Government of India (Grant No. SR/S3/CE/14/2005-SERC-Engg).

References

[1] J.S. Blakemore. Semiconducting and other major properties of gallium arsenide. *J. Appl. Phys.*, **53**(10), R123 (1982).
[2] J. Tersoff. New empirical model for the structural properties of silicon. *Phys. Rev. Lett.*, **56**(6), 632 (1986).
[3] J. Tersoff. New empirical approach for the structure and energy of covalent systems. *Phys. Rev. B*, **37**(12), 6991 (1988).
[4] J. Tersoff. Modeling of solid state chemistry: interatomic potentials for multicomponent systems. *Phys. Rev. B*, **39**(8), 5566 (1989).
[5] W.H. Moon, J. Hwang. Structural and thermodynamic properties of GaN: a molecular dynamics simulation. *Phys. Lett. A*, **315**, 319 (2003).
[6] M.B.K. Souraya Goumri-Said, A.E. Merad, H.A. Ghouti Merad. Prediction of structural and thermodynamic properties of zinc-blende AlN: molecular dynamics simulation. *Chem. Phys.*, **302**, 135 (2004).
[7] F. Benkabou, Z. Chelahi Chikr, H. Aourag, P.J. Becker, M. Certier. Atomistic study of zinc-blende BAs from molecular dynamics. *Phys. Lett. A*, **252**, 319 (1999).
[8] P.A. Ashu, J.H. Jefferson, A.G. Cullis, W.E. Hagston, C.R. Wlhitehouse. Molecular dynamics simulation of (100) InGaAs/-GaAs strained-layer relaxation processes. *J. Cryst. Growth*, **150**, 176 (1995).
[9] M. Nakamura, H. Fujioka, K. Ono, M. Takeuchi, T. Mitsui, M. Oshima. Molecular dynamics simulation of III–V compound semiconductor growth with MBE. *J. Cryst. Growth*, **209**, 232 (2000).
[10] S.I. Novikova. Properties of gallium arsenide. *Sov. Phys. Solid State*, **3**, 129 (1961).
[11] J. Adhikari, D. A. Kofke. Molecular simulation study of miscibility of ternary and quaternary InGaAlN alloys. *J. Appl. Phys.*, **95**(11), 6129 (2004).
[12] J. Adhikari, D. A. Kofke. Molecular simulation study of miscibility in $In_xGa_{1-x}N$ ternary alloys. *J. Appl. Phys.*, **95**(8), 4500 (2004).
[13] K. Nordlund, J. Nord, J. Frantz, J. Keinonen. Strain-induced Kirkendall mixing at semiconductor interfaces. *Comput. Mater. Sci.*, **18**(3–4), 283 (2000).
[14] S. Massidda, A. Continenza, A.J. Freeman, T.M. de Pascale, F. Meloni, M. Serra. Structural and electronic properties of narrow-band-gap semiconductors: InP, InAs, and InSb. *Phys. Rev. B*, **41**(17), 12079 (1990).
[15] P.W. Sparks, A. Swenson. Thermal expansions from 2 to 40°K of Ge, Si, and four III–V compounds. *Phys. Rev.*, **163**, 779 (1967).
[16] J.C. Mikkelsen, B. Boyce. Atomic-scale structure of random solid solutions: extended X-ray-absorption fine-structure study of Ga1-xInxAs. *Phys. Rev. Lett.*, **49**(19), 1412 (1982).